PAPER • OPEN ACCESS

A robust firearm identification algorithm of forensic ballistics specimens

To cite this article: Z L Chuan *et al* 2017 *J. Phys.: Conf. Ser.* **890** 012126

View the article online for updates and enhancements.

IOP ebooks™

Bringing you innovative digital publishing with leading voices to create your essential collection of books in STEM research.

Start exploring the collection - download the first chapter of every title for free.

A robust firearm identification algorithm of forensic ballistics specimens

Z L Chuan[1], A A Jemain[2], C-Y Liong[2], N A M Ghani[3] and L K Tan[4]

[1] Faculty of Industrial Sciences & Technology, Universiti Malaysia Pahang, Lebuhraya Tun Razak, 26300 Gambang Kuantan, Pahang DM, Malaysia
[2] School of Mathematical Sciences, Faculty of Science and Technology, Universiti Kebangsaan Malaysia, 43600 UKM Bangi, Selangor DE, Malaysia
[3] Centre of Statistical and Decision Science Studies, Faculty of Computer and Mathematical Sciences, Universiti Teknologi MARA, 40450 Shah Alam, Selangor DE, Malaysia
[4] Department of Mechanical Precision Engineering, Malaysia-Japan International Institute of Technology, Universiti Teknologi Malaysia, UTM KL, Jalan Sultan Yahya Petra, 54100 Kuala Lumpur, Malaysia

Email: chuanzunliang@ump.edu.my

Abstract. There are several inherent difficulties in the existing firearm identification algorithms, include requiring the physical interpretation and time consuming. Therefore, the aim of this study is to propose a robust algorithm for a firearm identification based on extracting a set of informative features from the segmented region of interest (**ROI**) using the simulated noisy center-firing pin impression images. The proposed algorithm comprises Laplacian sharpening filter, clustering-based threshold selection, unweighted least square estimator, and segment a square **ROI** from the noisy images. A total of 250 simulated noisy images collected from five different pistols of the same make, model and caliber are used to evaluate the robustness of the proposed algorithm. This study found that the proposed algorithm is able to perform the identical task on the noisy images with noise levels as high as 70%, while maintaining a firearm identification accuracy rate of over 90%.

1. Introduction

Firearm examiners are able to identify the type and the model of firearms that is being used by criminal via the cartridge cases discovered at the crime scene. The traditional firearm identification technique used in forensic laboratories is performed by using comparison microscope [1]. However, this traditional firearm identification technique is heavily dependent on the expertise and experience of the firearm examiners and time consuming. Moreover, the comparison process typically involves the cartridge cases manufactured by thousands agencies located in a broad geographical area. Therefore, the firearm identification by using a traditional firearm identification technique becomes tedious and difficult tasks when the database of evidence material grew large.

After the advent of ballistic identification systems in the past decades such as DRUGFIRE system, IBIS system, FIREBALL system, the French CIBLE system and the Russian TAIS system [2], the comparing process for traditional firearm identification technique can be performed automatically, namely image matching. These ballistic identification systems are able to create a short list that shows similarities between the characteristic impressions form on the cartridge cases discovered at the crime scene and the prototype 2D or 3D images stored in the database of these ballistic imaging systems. Although the ballistic identification systems are more efficient compared to the traditional firearm identification technique, however, the fundamental difficulty remains unsolved as the matching results provided by the ballistic identification systems are still dependent on the expertise and experience of

firearm examiners for verification. In addition, tuning the shape and position of the characteristic impression images by manually is indeed much needed during the data acquisition process [3].

Besides the aforementioned ballistic imaging systems, researchers also have been proposed several algorithms for firearm identification based on cartridge case images in order to further improve and developed a sophisticated algorithm for firearm identification without depending on physical interpretation [4-8]. The proposed algorithms comprise three main components, namely image preprocessing, feature extraction and identification. Image preprocessing is to ensure that the resultant image is more suitable to be used for further processing compared to the input image. At this stage, the input image is applied to various appropriate operations such as image enhancement, noise removal and segmentation. Since there is no general theory to determine the best image enhancement and segmentation operation for specific applications, trial and error approach is indeed much needed in order to obtain an appropriate operation [9]. The stage after image preprocessing is feature extraction. The aim of features extraction is to represent and aggregate the image or segmented certain region of cartridge case image that defined as the region of interest (**ROI**), in terms of quantifiable measurement, which will be more easily used in the identification stage. On the identification stage, the classifier is used to identify the type and the model of firearm that discharged the cartridge case based on the extracted features.

Based on previously proposed algorithms, features can be extracted from the cartridge case image with or without segmentation of the characteristic impressions such as firing pin impression, breech face impression and the ejector impression as illustrated in Figure 1. Features extracted from segmented characteristic impressions are more advantageous than without segmentation in terms of computational cost and execution time. This is due to the involvement of the smaller array of raw data set. However, only a few previously proposed algorithms extract features from segmented characteristic impressions based on determining the position of characteristic impressions on the cartridge case. Xin et al. [4] proposed extracting several separable features from the firing pin impression, breech face impression and ejector impression. Before segmenting the key impressions, Xin's algorithm used the Hough transform method to determine the position of the character impressions. Zhou et al. [5] proposed extracting features from the firing pin and the breech face impression by using Active Snake Model and Local Orientation Analysis. Zhou's study also used the Hough transform method to determine the position of the characteristic impression. Meanwhile, Li [6] proposed determining the position of the firing pin impression and the boundary of the cartridge case by using the direct least squares fitting of ellipses approach. However, feature extraction is not presented in Li's study. Recently, Ghani et al. [7] and Kamaruddin et al. [8] proposed determining the position of the center-firing impression manually. In their studies, the features are extracted from the center-firing pin impression using geometric moments.

In general, the firing pin impression can be categorized into two kinds, namely rim-firing pin impression and center-firing pin impression. The characteristic impression focused on this study is the center-firing pin impression as well as it was robust in firearm identification rather than breech impression and ejector impressions. This is due to the center-firing pin impression always appears like a small cave on cartridge cases, while breech face and ejector impression are very difficult to observe [3,7]. The purpose of this study is to propose a robust algorithm for firearm identification by using noisy center-firing impression images. In addition, a comparative efficiency of the proposed algorithm, which applied with noise removals by using various window sizes in order to suppress the noise contaminated in the images are also presented. The rest of this study is organized as follows. In Section 2 and Section 3, descriptions of impulse noise and noise removals are presented, respectively. The procedure to perform the proposed segmentation algorithm is rendered in Section 4 while experimental results are discussed in Section 5. Finally, Section 6 concludes this study.
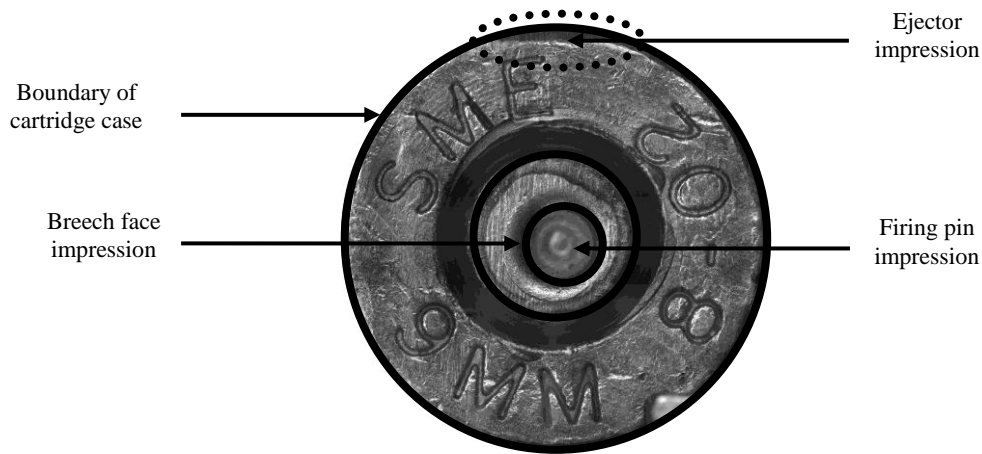
Figure 1. The common key impressions that were the focus in previous algorithms.

2. Background of impulse noise model

Impulse noise can be introduced into digital image via the transmission errors, malfunctioning pixel elements in the camera sensors, faulty memory locations, and timing errors in analog-to-digital conversion [10]. In general, there are two typical additive impulse noises can be introduced into a digital image, which are fixed-valued (salt and pepper noise) and random-valued impulse noise (uniform noise). However, this study focused on random-valued impulse noise only. Denoted $\mathbf{D} = [f(x, y)]_{M \times N}$ represents an uncontaminated center-firing pin impression image of the size $M \times N$ with pixel value $f \in \{a/255; a = 0, 1, 2, \ldots, 255\}$ located at (x, y) in the image $\mathbf{D}$, where $x, (y) = 0, 1, 2, \ldots, M-1, (N-1)$. When the image $\mathbf{D}$ is contaminated with random-valued impulse noise at the noise level, $p(100)\%$, the image $\mathbf{D}$ becomes a noisy image, namely $\mathbf{D_n} = [f_{\mathbf{n}}(x, y)]_{M \times N}$, where $f_{\mathbf{n}}(x, y)$ is defined as below.

$$f_{\mathbf{n}}(x, y) = \begin{cases} f(x, y), & 1 - p \\ n(x, y), & p \end{cases} \tag{1}$$

where $0 < p < 1$ is the noise ratio and n represents the intensity of the noisy pixel. In other words, the n is a random-valued impulse noise that is uniformly distributed in the dynamic range of f. In this study, the noise ratio has been used to evaluate the robustness of the proposed algorithm for firearm identification is $p = [0.1, 0.7]$ as illustrated in Figures. 2(b)-(h), respectively. The procedure for simulating $p(100)\%$ random-valued noise in order to contaminate the image $\mathbf{D}$ is explained explicitly in the following step.

Step 1. Input an image $\mathbf{D}$ as illustrated in Figure 2(a) into the R statistical software.
Step 2. Generate a set of random $p \times MN$ coordinate points, (x, y), and $p \times MN$ intensity, n, which uniformly distributed in the dynamic range of f. Hence, $n(x, y)$ is resulted.
Step 3. Replace the $f(x, y)$ in the image $\mathbf{D}$ with $n(x, y)$ according to the (x, y) generated in Step 2. Therefore, the image $\mathbf{D_n}$ at noise ratio $p = [0.1, 0.7]$ is resulted as illustrated in Figures. 2(b)-(h) respectively.
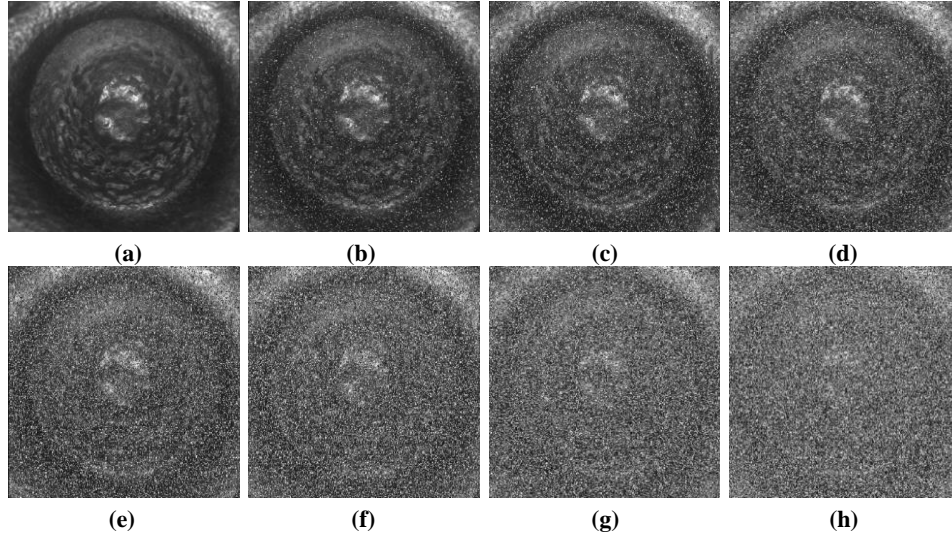
Figure 2. (a) Original image (b), (c), (d), (e), (f), (g), (h), (i), (j) is the image contaminated with random-valued impulse noise at noise ratio, $p = [0.1, 0.7]$ respectively.

3. Background of noise removals

De-noising the image $\mathbf{D_n}$ contaminated with random-valued impulse noise can be performed by applying smoothing spatial filters (SSF). In this study, median and midpoint smoothing spatial filters are applied in the image $\mathbf{D_n}$. Median smoothing spatial filter (MeSSF) is a well-known nonlinear filtering method, with the potential to suppress noise with high computational efficiency and has been successfully applied to many signal and image processing tasks [10,11]. In other respects, previous study [12] showed that midpoint smoothing spatial filter (MpSSF) is another effective filtering method that is able to suppress the random-valued impulse noise. Therefore, both MeSSF and MpSSF are applied in this study and the effectiveness of both SSF are compared. Consider $\mathbf{S}$ is the sub-image for an image $\mathbf{D_n}$ with window size $(2b+1) \times (2b+1)$ as denoted below.

$$\mathbf{S} = \begin{bmatrix} f_\mathbf{n}(x-b, y+b) & \cdots & f_\mathbf{n}(x+0, y+b) & \cdots & f_\mathbf{n}(x+b, y+b) \\ \vdots & \ddots & \vdots & \cdot^{\cdot^{\cdot}} & \vdots \\ f_\mathbf{n}(x-b, y+0) & \cdots & f_\mathbf{n}(x+0, y+0) & \cdots & f_\mathbf{n}(x+b, y+0) \\ \vdots & \cdot^{\cdot^{\cdot}} & \vdots & \ddots & \vdots \\ f_\mathbf{n}(x-b, y-b) & \cdots & f_\mathbf{n}(x+0, y-b) & \cdots & f_\mathbf{n}(x+b, y-b) \end{bmatrix} \tag{2}$$

where $b = 1, 2, \ldots, \dfrac{N-1}{2}$. All centered intensity of $\mathbf{S}$, $f_\mathbf{n}(x+0, y+0)$, are replaced with median value, $f_{med}(x, y)$, and midpoint value, $f_{mp}(x, y)$, after the image $\mathbf{D_n}$ has been applied with MeSSF and MpSSF, respectively.

$$f_{med}(x, y) = \text{median}\big[\text{vec}(\mathbf{S}) \big] \tag{3}$$

$$f_{mp}(x, y) = \big\{ \max\big[\text{vec}(\mathbf{S}) \big] + \min\big[\text{vec}(\mathbf{S}) \big] \big\} \big/ 2 \tag{4}$$

The $\mathrm{vec}(\mathbf{S})$ represents the vectorization of the sub-image, $\mathbf{S}$.

4. Proposed algorithm
This section describes the procedures for implementing the proposed algorithm for firearm identification. The proposed algorithm is explained explicitly in the following steps.

4.1. Image enhancement, noise removal and segmentation

Step 4.   Apply Laplacian sharpening filter ($\mathbf{L}$) to the image $\mathbf{D_n}$ to enhance the edge of the center-firing pin impression. As a result, the suitable sharpening spatial filters for specific applications are determined empirically. The $\mathbf{L}$ is selected as well as it successfully applied in previous studies [13,14]. A new image, $\mathbf{D_{nL}} = \left[f_{nL}(x,y) \right]_{(M-2)\times(N-2)}$, is produced after $f_n(x+0, y+0)$ for $\mathbf{S}$ is replaced with the gradient, $f_{nL}(x,y)$, computed based on the following equation.

$$f_{nL}(x,\, y) = 255\,\mathrm{vec}(\mathbf{T_L})^T\,\mathrm{vec}(\mathbf{S}) \tag{5}$$

where $\mathbf{T_L} = \begin{bmatrix} 0 & 1 & 0 \\ 1 & -4 & 1 \\ 0 & 1 & 0 \end{bmatrix}$ is the kernel for $\mathbf{L}$, $f_{nL} \in [-\infty, \infty]$.

Step 5.   Compress the dynamic range for f_{nL} by using histogram normalization due to the dynamic range resulted in Step 4 is outside the dynamic range of f. The compression of dynamic range is performed using the function below.

$$f_{nN}(x,y) = \left\lfloor \left(f_{nL} - \max f_{nL}\right)\big/\left(\max f_{nL} - \min f_{nL}\right)\times 255 \right\rfloor \Big/ 255 \tag{6}$$

where $\min f_{nL}$ and $\max f_{nL}$ represent the minimum and the maximum intensities for image $\mathbf{D_{nL}}$, respectively. A new image, $\mathbf{D_{nN}} = [f_{nN}(x,y)]_{(M-2)\times(N-2)}$, is resulted with the floor intensity, $f_{nN} \in \{a/255; a = 0,\ 1,\ 2,\ \dots,\ 255\}$, after the dynamic range is compressed. The floor function, $\lfloor \cdot \rfloor$, is selected rather than rounding the numerator directly into integer since higher firearm identification accuracy rates is resulted when a floor function is used, while there is no significant difference in the execution time for the algorithm which applied with floor function and rounding off the numerator directly into an integer.

Step 6.   Binarize the image $\mathbf{D_{nN}}$ by using thresholding. The firing pin impression can be isolated completely from its background when an appropriate threshold is selected. In this study, clustering-based threshold selection method proposed by Otsu [15] is selected. Clustering-based threshold selection method is promising due to its effective results in most image processing applications [3,16-18]. An optimal threshold, $\tilde{t}$, is determined by maximizing the following criterion function:

$$\tilde{t} = \arg\left(\max_t \left[\left(\mu_{255} - \mu_t\right)^2 \left(\varphi_t/(1-\varphi_t)\right) \right] \right)\Big/255 \tag{7}$$

where

$$\pi_{\mathbf{nN}}(g) = \left(\sum_{x,y}^{M-2,N-2} \mathrm{I}\left(f_{\mathbf{nN}}(x,y) = 255g\right) \right) \Bigg/ (M-2)(N-2), \quad \mu_{255} = \sum_{a=0}^{255} 255g\,\pi_{\mathbf{nN}}(a),$$

$$\mu_t = \sum_{a=0}^{t} 255g\,\pi_{\mathbf{nN}}(a), \quad \varphi_t = \sum_{a=0}^{t} \pi_{\mathbf{nN}}(a), \quad \mathrm{I}(\cdot) \text{ represents the indicator function.}$$

A binary image, $\mathbf{D_{nB}} = [f_{\mathbf{nB}}(x,y)]_{(M-2)\times(N-2)}$, is produced after applying the clustering-based threshold selection method, whereby $f_{\mathbf{nB}} = \begin{cases} 0, & f_{\mathbf{nN}} < \tilde{t} \\ 1, & f_{\mathbf{nN}} \geq \tilde{t} \end{cases}$.

Step 7.   Estimate the anchor point, $\mathbf{A} = (X_{\mathbf{C}}, Y_{\mathbf{C}})^T$ and radius of the firing pin impression, r, by using the unweighted least square estimator [19]. The unweighted least square estimator is preferred due to it was the simplest and incurred the least execution time compared to the weighted least square estimator [20], Hough transform [21] and direct least square fitting of ellipses approach [22]. The $\mathbf{A}$ and r can be estimated by using equations (8) and (9), respectively.

$$\mathbf{A} = \begin{bmatrix} 2\left(h\beta_{20} - \beta_{00}\beta_{10}^2\right) & 2\left(h\beta_{11} - \beta_{10}\beta_{01}\right) \\ 2\left(h\beta_{11} - \beta_{10}\beta_{01}\right) & 2\left(h\beta_{02} - \beta_{00}\beta_{01}^2\right) \end{bmatrix}^{-1} \begin{bmatrix} h(\beta_{30} + \beta_{12}) - \beta_{10}(\beta_{20} + \beta_{02}) \\ h(\beta_{03} + \beta_{21}) - \beta_{01}(\beta_{20} + \beta_{02}) \end{bmatrix} \quad (8)$$

$$r = \sqrt{\left(\sum_{x,y}^{M-2,N-2} \left((X_{\mathbf{C}} - x^2) + (Y_{\mathbf{C}} - y)^2 \right) \right) \Bigg/ (M-2)(N-2)} \quad (9)$$

where $\beta_{ij} = \sum_{x,y}^{M-2,N-2} x^i y^j f_{\mathbf{nB}}(x,y)$ and $h = \sum_{x,y}^{M-2,N-2} f_{\mathbf{nB}}(x,y)$.

Step 8.   Remove the noise in the contaminated image, $\mathbf{D_n}$ by applying the MeSSF and MpSSF. The window sizes, $b = [0,7]$ for the filter is used. Therefore, a new image, $\hat{\mathbf{D}} = [\hat{f}(x,y)]_{M \times N}$ is resulted, where $\hat{f} \in \{a/L; a = 0, 1, 2, \ldots, L = 255\}$.

Step 9.   Segment the **ROI** from the $\hat{\mathbf{D}}$ based on the estimated $\mathbf{A}$ and r. Since the **ROI** is segmented using square form, it can be defined as $\mathbf{ROI} = \left[\hat{f}(x_1, y_1) \right]_{r/4 \times r/4}$, whereby $x_1,(y_1) = 0, 1, 2, \ldots, r/4-1,(r/4-1)$. Segmenting the **ROI** by using square is preferred due to it is more efficient compared to a circular form.

4.2. Feature extraction and identification

Step 10.   Extract the features from the segmented **ROI**. The features set, namely orthogonal Legendre moments are extracted from **ROI** based on previous study [23], which can be calculated by using the following function.

$$\lambda_{uv} = \left\{ (2p+1)(2q+1) \sum_{k=0}^{u} \sum_{l=0}^{v} c_{uk} c_{lv} m_{kl} \right\} \Bigg/ 4, \quad k,l = 0, 1, 2,\ldots \quad (10)$$

where

$$c_{uk} = \begin{cases} \left((-1)^{(u-k)/2}(u+k)!\right)\Big/\left(2^u k!\left((u-k)/2\right)!\left((u+k)/2\right)!\right), & (u-k) \text{ even} \\ 0, & (u-k) \text{ odd} \end{cases};$$

$$m_{kl} = \sum_{x_1}\sum_{y_1}\left(4x_1/r - 1\right)^k \left(4y_1/r - 1\right)^l f\left(x_1, y_1\right) \quad u, v = 0, 1, 2, \ldots$$

Seven orthogonal Legendre moments provide features for identification, namely λ_{10}, λ_{11}, λ_{20}, λ_{02}, λ_{12}, λ_{21}, and λ_{22}, which are selected based on stepwise feature selection [23].

Step 11. Identify the type of firearm by using Fisher linear discriminant analysis [24]. Input the selected informative features set into the classifier and the firearm identification accuracy rate is resulted.

Step 12. Steps 1 to 11 are repeated 10 times for all levels of noise. Therefore, 10 accuracy rate readings are resulted for each level of noise and window size.

5. Simulation results and discussion

There are 250 uncontaminated center-firing pin impression images collected from 5 pistols of the model Parabellum Vektor SP1 9mm, which are labeled with Pistol 1, Pistol 2, Pistol 3, Pistol 4 and Pistol 5 as the sample images illustrated in Figure 3. The five pistols selected have the same make, model and caliber with the assumption that all five pistols selected are able to produce different individual characteristic, namely firing pin impression. However, the differences of the individual characteristic formed on the cartridge cases were difficultly distinguished by firearm examiners. In other respects, the pistols with caliber 9mm are selected since this pistol was the type of firearms, which typically used by criminal in Malaysia. All the cartridge cases used are manufactured in the year 2002 and also have the similar lot number.

This study defines that the proposed algorithm is robust if the resulting average of firearm identification accuracy rate is more than 90%, and the accuracy rate of the algorithm applying SSF is always significantly higher compared to without applying SSF for any given noise level. The average of firearm identification accuracy rate for the algorithm, which used radius $r/4$ in order to segment the **ROI** and without applied with smoothing spatial filters at noise ratio, $p = 0.1$ is 94.40% [(94.80%+94.80%+94.80%+94.00%+94.40%+94.40%+94.00%+93.60%+94.40%+94.80%)/10] with standard deviation, $\sigma = 0.42$. Based on the simulation results shown in Table 1, this study found that without applying filters, the proposed algorithm can perform efficiently at noise levels as high as 70% In practice, the type of additive noise that contaminates the images can be detected via the histogram of the image. On the other hands, previous studies [25,26] also proposed methods which were able to detect the candidates for additive noise in an image. However, these proposed methods failed to estimate the noise levels accurately. Therefore, smoothing spatial filters that are able to remove the noise are needed when an image has been contaminated with random-valued impulse noise for all noise levels.

In Table 1, the firearm identification accuracy rates in bold for different sizes of filters represent the accuracy rate is significantly higher than the algorithm without a filter. The simulation results show that the accuracy rate of the algorithm applied to MpSSF filter is always significantly lower than the accuracy rate of the algorithm without a filter. Therefore, this study concludes that the MpSSF is not ideal to remove the random-valued impulse noise. Furthermore, Table 1 also shows that the algorithm applied MeSSF with window sizes of 11×11, 13×13 and 15×15 are always robust when the images are contaminated by random-valued impulse noise at levels as high as 70%. However, the imposed execution time is longer when the window size of the filter is larger. This is due to the larger

the window sizes of the filter, the larger the number of data involved. Consequently, the sorting process for the median takes a long time. Based on these analyses, this study concludes that with a random-valued impulse noise levels as high as 70%, the proposed algorithm is robust when applied to the median filter of window size 11x11.
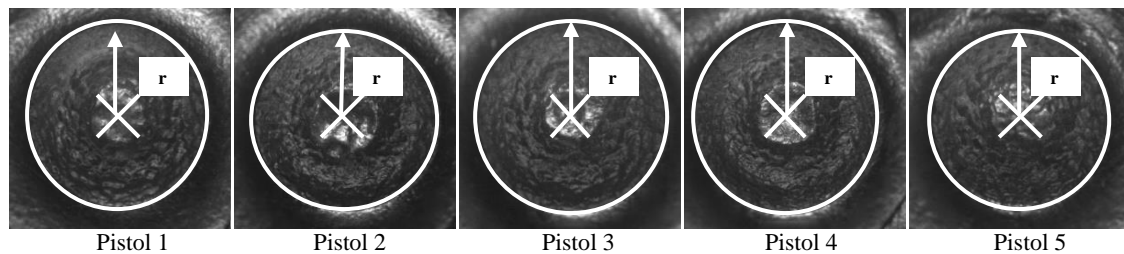

| Pistol 1 | Pistol 2 | Pistol 3 | Pistol 4 | Pistol 5 |

Figure 3. Sample images of firing pin impression for Pistol 1, Pistol 2, Pistol 3, Pistol 4 and Pistol 5.

Table 1. Average of firearm identification accuracy rate (standard deviation).

Filter	Window size	Noise Added (%)						
		10	20	30	40	50	60	70
Without filtering	-	94.40 (0.42)	93.96 (0.64)	94.00 (0.46)	93.76 (0.85)	93.48 (0.82)	93.20 (1.21)	91.64 (1.34)
Median filtering	3×3	94.64 (0.28)	**94.56*** **(0.54)**	**94.52*** **(0.42)**	**94.40*** **(0.50)**	93.92 (0.49)	**94.24*** **(0.71)**	**93.52*** **(1.16)**
	5×5	94.60 (0.34)	94.36 (0.40)	94.32 (0.53)	**94.48*** **(0.53)**	**94.24*** **(0.28)**	**94.20*** **(0.54)**	**93.44*** **(0.57)**
	7×7	94.52 (0.42)	94.28 (0.50)	94.44 (0.58)	**94.36*** **(0.35)**	94.12 (0.33)	**94.24*** **(0.63)**	**93.84*** **(0.74)**
	9×9	94.88 (0.32)	**94.88*** **(0.41)**	94.32 (0.56)	**94.32*** **(0.32)**	93.84 (0.54)	**94.72*** **(0.67)**	**93.92*** **(0.86)**
	11×11	**95.24*** **(0.44)**	**94.92*** **(0.46)**	**95.00*** **(0.34)**	**94.56*** **(0.47)**	**94.24*** **(0.43)**	**94.76*** **(0.55)**	**93.52*** **(0.59)**
	13×13	**95.56*** **(0.55)**	**95.20*** **(0.27)**	**94.96*** **(0.54)**	**94.56*** **(0.51)**	**94.44*** **(0.74)**	**94.64*** **(0.74)**	**94.80*** **(0.82)**
	15×15	**95.80*** **(0.34)**	**95.36*** **(0.39)**	**95.04*** **(0.47)**	**94.92*** **(0.38)**	**94.88*** **(0.49)**	**94.96*** **(0.93)**	**93.96*** **(0.55)**
Midpoint filtering	3×3	93.56* (0.83)	93.12* (0.75)	90.76* (1.39)	88.00* (0.73)	85.20* (1.73)	79.36* (2.19)	73.40* (2.75)
	5×5	90.76* (1.40)	83.36* (2.49)	73.96* (2.25)	65.32* (2.28)	57.64* (3.00)	51.40* (2.63)	46.92* (2.76)
	7×7	83.56* (1.64)	69.40* (2.69)	59.48* (2.52)	55.84* (2.25)	49.92* (1.34)	48.52* (2.33)	42.92* (3.47)
	9×9	73.76* (3.20)	60.44* (3.54)	56.92* (3.10)	53.96* (2.66)	49.68* (2.16)	44.88* (1.06)	43.56* (1.90)
	11×11	68.16* (2.42)	57.60* (2.69)	54.56* (2.65)	51.56* (2.22)	51.36* (2.73)	48.76* (2.98)	45.60* (2.00)
	13×13	60.36* (3.52)	56.52* (3.27)	54.72* (4.13)	54.48* (3.06)	52.40* (4.34)	48.04* (3.57)	46.20* (3.75)
	15×15	58.80* (3.89)	57.68* (1.97)	56.64* (5.70)	52.76* (4.48)	51.00* (3.68)	50.48* (2.40)	45.68* (1.69)

*Note: Asterisk(*) represents a significant difference between the mean of accuracy rate for an image with filtering and without filtering at a significance level of $\alpha = 0.05$.

6. Conclusion and future work

An efficient algorithm for firearm identification is introduced. The simulation results show that the median filter with the optimal window size of 11×11 is the ideal filter to enhance images contaminated with random-valued impulse noise. This study concludes that the proposed algorithm for firearm identification is robust when the images are contaminated with random-valued impulse noise with levels as high as 70%. In the forthcoming papers, the study will introduce more sophisticated filters such as switching median filter, multistate median filter and adaptive center filter, weighted

median filter to investigate a more efficient filter that is able to remove the noise with levels as high as 90%.

References

[1]   De Kinder J, Tulleners F and Thiebaut H 2004 Reference ballistic imaging database performance *Forensic Science International* **140**(2-3) 207-215.

[2]   Geradts Z J, Bijhold J, Hermsen R and Murtagh F 2001 Image matching algorithms for breech face marks and firing pins in a database of spent cartridge cases of firearms *Forensic Science International* **119**(1) 97-106.

[3]   Leng J and Huang Z 2012 On analysis of circle moments and texture features for cartridge images Recognition *Expert Systems with Applications* **39**(2) 2092-2101.

[4]   Xin L-P, Zhou J and Rong G 2000 A cartridge identification system for firearms authentication *Proceedings of the IEEE Signal Processing* pp. 1405-1408.

[5]   Zhou J, Xin L-P, Gao D-S, Zhang C-S and Zhang D 2001 Automated cartridge identification for firearms authentication *Proceedings of the IEEE Computer Society Conference* pp.749-754.

[6]   Li D G 2003 Image processing for the positive identification of forensic ballistics specimens *Proceedings of the 6th International Conference on Information Fusion* pp.1494-1498.

[7]   Ghani N A M, Liong C-Y and Jemain A A 2010 Analysis of geometric moments as features for firearm identification *Forensic Science International* **198**(1-3) 143-149.

[8]   Kamaruddin S B A, Ghani N A M, Liong C-Y and Jemain A A 2011 Firearm recognition based on whole firing pin impression image via backpropagation neural network *Proceedings of the IEEE International Conference on Pattern Analysis and Intelligent Robotics* pp. 177-182.

[9]   Shih F Y 2010 *Image Processing and Pattern Recognition: Fundamentals and Techniques* (Hoboken: John Wiley & Sons).

[10]   Bovik A C, Huang T S and Munson D C 1987 The effect of median filtering on edge estimation and detection *IEEE Transactions on Pattern Analysis and Machine Intelligence* **PAMI-9**(2) 181-194.

[11]   Chan R H, Ho C-W and Nikolova M 2005 Salt-and-pepper noise removal by median-type noise detectors and detail-preserving regularization *IEEE Transactions on Image Processing* **14**(10) 1479-1485.

[12]   Srinivasan E and Ebenezer D 2008 New nonlinear filtering strategies for eliminating short and long tailed noise in images with edge preservation properties *International Journal of Information and Communication Engineering* **4**(3) 175-181.

[13]   Chuan Z L, Jemain A A, Liong C-Y and Ghani N A M 2013 Effectiveness of Cross-Entropy and Tsallis Entropy thresholding for automatic forensic ballistics identification system *Journal of Quality Measurement and Analysis* **9**(1) 33-46.

[14]   Chuan Z L, Liong C-Y, Jemain A A and Ghani N A M 2013 Automatic anchor point detection approach for firearms firing pin impression *Sains Malaysiana* 42(9) 1339-1344.

[15]   Otsu N 1979 A threshold selection method from gray-level histograms *IEEE Transactions on Systems, Man, and Cybernetic* **SMC-9**(1) 62-66.

[16]   Chen H and Gururajan R 2011 A de-noising method for heart sound signal using Otsu's
        threshold selection. In *Proceedings of IET International Communication Conference
        on Wireless Mobile and Computing* pp. 65-69.
[17]   Gupta M R, Jacobson N P and Garcia E K 2007 OCR binarization and image pre-processing
        for searching historical documents *Pattern Recognition* **40**(2) 389-397.
[18]   Lin Z and Yu H 2011 The pupil location based on the OTSU method and hough transform
        Procedia Environmental Sciences **8** 352-356.
[19]   Moura L and Kitney R 1991 A direct method for least-squares circle fitting *Computer Physics
        Communications* **64**(1) 57-63.
[20]   Albano A 1974 Representation of digitized contours in terms of conic arcs and straight-line
        segments *Computer Graphics and Image Processing* **3** 23-33.
[21]   Yuen H K, Princen J, Illingworth J and Kittler J 1990 Comparative study of Hough Transform
        methods for circle finding *Image and Vision Computing* **8**(1) 71-77.
[22]   Fitzgibbon A, Pilu M and Fisher R B 1999 Direct least squares fitting of ellipses. *Proceedings
        of the 13th International Conference on Pattern Recognition*, pp. 253-257.
[23]   Ghani N A M, 2010 *Analysis of Forensic Ballistics Specimens for Firearm Recognition*, Ph.D.
        thesis, School of Mathematical Sciences, Universiti Kebangsaan Malaysia.
[24]   Fisher R A 1936 The use of multiple measurements in taxonomic problems *Annals of
        Eugenics* **7**(2) 179-188.
[25]   Dong Y, Chan R H and Xu S 2007 A detection statistic for random-valued impulse noise
        IEEE Transactions on Image Processing **16**(4) 1112-1120.
[26]   Garnett R, Huegerich T, Chui C and W. He 2005 A universal noise removal algorithm with an
        impulse detector *IEEE Transactions on Image Processing* **14**(11) 1747-1754.